Biodegradation (2011) 22:773–795
DOI 10.1007/s10532-010-9434-0

ORIGINAL PAPER

Molecular assessment of microbiota structure and dynamics along mixed olive oil and winery wastewaters biotreatment

Ana Eusébio · Marta Tacão · Sandra Chaves · Rogério Tenreiro · Elsa Almeida-Vara

Received: 20 April 2010 / Accepted: 26 October 2010 / Published online: 11 November 2010

Abstract The major parcel of the degradation occurring along wastewater biotreatments is performed either by the native microbiota or by added microbial inocula. The main aim of this study was to apply two fingerprinting methods, temperature gradient gel electrophoresis (TGGE) and length heterogeneity-PCR (LH-PCR) analysis of 16S rRNA gene fragments, in order to assess the microbiota structure and dynamics during mixed olive oil and winery wastewaters aerobic biotreatment performed in a jet-loop reactor (JLR). Sequence homology analysis showed the presence of bacterial genera *Gluconacetobacter*, *Klebsiella*, *Lactobacillus*, *Novosphingobium, Pseudomonas*, *Prevotella*, *Ralstonia*, *Sphingobium* and *Sphingomonas* affiliated with five main phylogenetic groups: alpha-, beta- and gamma-Proteobacteria, Firmicutes and Bacteroidetes. LH-PCR analysis distinguished eight predominant DNA fragments correlated with the samples showing highest performance (COD removal rates of 67 up to 75%). Cluster analysis of both TGGE and LH-PCR fingerprinting profiles established five main clusters, with similarity coefficients higher than 79% (TGGE) and 62% (LH-PCR), and related with hydraulic retention time, indicating that this was the main factor responsible for the shifts in the microbiota structure. Canonical correspondence analysis revealed that changes observed on temperature and O_2 level were also responsible for shifts in microbiota composition. Community level metabolic profile analysis was used to test metabolic activities in samples. Integrated data revealed that the microbiota structure corresponds to bacterial groups with high degradative potential and good suitability for this type of effluents biotreatments.

Keywords Microbiota structure · Microbiota dynamics · Microbiota diversity · TGGE · LH-PCR · Olive oil wastewater · Winery wastewater

A. Eusébio (✉) · M. Tacão
LNEG, Unidade de Bioenergia, Estrada do Paço do Lumiar, 22, 1649-038 Lisbon, Portugal
e-mail: ana.eusebio@lneg.pt

A. Eusébio · E. Almeida-Vara
Centro de Biodiversidade, Genómica Integrativa e Funcional (BioFIG), FCL, C2, Campo Grande, 1749-016 Lisbon, Portugal

S. Chaves · R. Tenreiro
Universidade de Lisboa, Faculdade de Ciências, Centro de Biodiversidade, Genómica Integrativa e Funcional (BioFIG), Edifício ICAT, Campus da FCUL, Campo Grande, 1749-016 Lisbon, Portugal

Introduction

Industrial effluent treatment and discharge is a worldwide concern with economical, social and environmental repercussions. Nowadays, environmental regulations are more and more demanding,

compelling the industry to develop efficient treatment technologies.

The present work is a case study reporting the biological aerobic treatment using a jet-loop reactor (JLR) of mixed olive oil wastewaters (OOWW) and winery wastewaters (WW), two agro-industries of major importance to Portuguese Economy and also responsible for the production of very recalcitrant effluents with a strong negative impact in the environment.

Microorganisms have an essential role in the natural recycling and decomposition of materials and organic residues and thus native microbiota, or microbial in vitro developed inocula, used as biologic agent to treat wastewaters, has the great advantage to be ancestrally adapted to its natural environment (e.g. effluents) and that adaptation ability further determined its ultimate survival.

Among effluent treatment technologies, biological treatments carried out by aerobic or anaerobic reactors are often the choice of industrials because they are economic, easy to operate and can be designed to fit different spaces and volumes. Since bioreactor treatments depend mostly upon the microbiota ability to grow in this man-modified environment, the detailed assessment of structure, dynamics and function of the different microbiota populations present in that specific habitat, is the key issue to adjust that microbiota to natural or imposed environmental shifts, ensuring for the desired metabolic functions and the overall biotreatment efficiency.

However and in spite of the great expertise developed in biotreatment systems during several decades, microbiota "handling" achieved slight advances due to the limitation of the cultivation-dependent microbiology methods that do not necessarily provide consistent information on the composition of the entire microbiota. The molecular biology boom made available more accurate tools to highlight complex microbiota structure, dynamics and functions, as well as to detect microbiota members that are non-cultivable and therefore used to remain unknown ("silent" microorganisms, Smalla et al. 2008). Temperature gradient gel electrophoresis (TGGE) and length heterogeneity-PCR (LH-PCR) fingerprinting methods are very reliable to monitor shifts in microbiota composition, its dynamics and synergies, and the individual member's relative contribution either in natural habitats or in man-modified environments like soil bioremediation and effluent biotreatment (e.g. Bernhard et al. 2005; Díaz et al. 2006; Doaré-Lebrun et al. 2006; Henriques et al. 2006; Kirk et al. 2004; Kolehmainen et al. 2008; Liu et al. 2002; Moura et al. 2009; Muyzer and Smalla 1998; Rincón et al. 2006; Ritchie et al. 2000; Sousa et al. 2007; Talbot et al. 2008; Tiirola et al. 2003). Moreover, a great advantage of these methods is the possibility to evaluate and compare simultaneously a large number of multiple samples and in short time.

In addition, data obtained from TGGE and LH-PCR profiles can be analyzed by multivariate statistics and diversity indices, and obtained calculations give additional comparative information about the temporal and/or environmental changes of the microbiota during the biotreatment process (Talbot et al. 2008). Assuming that one operational taxonomic unit (OTU) corresponds to one species, richness of species, diversity Shannon index and evenness (or equitability) index can be calculated from fingerprints data to define the diversity of a microbiota (Eichner et al. 1999; Hill et al. 2003; Talbot et al. 2008).

Although the known limitations of culture-dependent methods, it is of most importance to characterize metabolic functions of a microbiota and to correlate shifts in its functional characteristics with changes in population structure or physiology. OOWW and WW are characterized by high organic matter concentration and the corresponding high levels of chemical oxygen demand (COD). Organic compounds present in these effluents include sugars, pectins, polyalcohols, anthocyanins, tannins, lipids, organic acids, amino acids and monomeric and polymeric aromatic molecules, generally referred as phenolic compounds (Borja et al. 2002; Colin et al. 2005; Di Gioia et al. 2001; El Hajjouji et al. 2008; Hamdi 1993; Kachouri and Hamdi 2004; Kiritsakis et al. 2001; Mekki et al. 2006; Piperidou et al. 2000). Due the diversity of organic compounds present in these effluents, it was expected that the corresponding microbial communities have the ability to use some of those compounds. An approach to differentiating the microbiota by its catabolic potential is the community level metabolic profile (CLPP) analysis that allows the characterization of the functional potential of the selected microbiota based on its ability to oxidize several carbon sources (Choi and Dobbs 1999; Garland and Mills 1991; Paixão et al. 2003).

Our previous work allowed a partial knowledge concerning OOWW and WW microbiota composition

with isolation and identification of the cultivable microorganisms and the optimization of JLR performance to increase treatment efficiency (Eusébio et al. 2004, 2005, 2007). The aim of this study is to analyse the microbiota composition (including cultivable and non-cultivable microorganisms) and its shifts along the biotreatment, in order to investigate the potential degradation roles of each group of microorganisms and/or of each microbial communities. For this purpose, an experiment was carried out in the JLR at the HRT of 6.0 days, insuring the good COD and phenolic compounds removal rates achieved in a previous OOWW treatment (Eusébio et al. 2007). Moreover, to mimic some of the constraints that are very often imposed to olive oil mills and wineries managers, namely the need to process higher volumes of effluents in short periods of time and also to treat mixes containing both effluents, a lower HRT of 4.5 days was tested as well as a mixture of OOWW with WW.

Materials and methods

Wastewaters sampling

Olive oil wastewater (OOWW) was obtained from the Olive oil mill at Pernes, and winery wastewater (WW) was collected from the co-operative winery at Olhalvo, Portugal. Raw effluents were transported to the laboratory in 800-l containers. A 25 l sample, from each effluent, was frozen at –20°C until further use. The remaining volume was kept in its container, at room temperature (RT), until the end of the respective biotreatment.

JLR setup and operation mode

The treatment was carried out using the JLR described in Eusébio et al. (2004). Wastewater biotreatment was performed along 25 days in the JLR with a working volume of 22.5 l, starting under a batch phase for 6 days using crude olive oil wastewater (OOWW1). After the acclimation step the continuous regimen was initiated with a feeding flow rate of 3.75 l day^{-1} followed 5.3 l day^{-1}, corresponding to the hydraulic retention times (HRT) of 6 and 4.5 days, and to the establishment of organic loads of 12.2 and 16.2 g COD l^{-1} day^{-1}, respectively. These settings were applied at 7th and 14th days of treatment. On the 18th day of treatment, the applied organic load was reduced to 8.7 g COD l^{-1} day^{-1} since new OOWW, from a second container preserved at RT (OOWW2), fed the bioreactor. After the 22nd day, WW was used to feed the JLR with the selected HRT of 6 days and the respective applied organic load of 4.8 g COD l^{-1} day^{-1}.

Sampling points

Samples were collected every 24 h from the JLR cylinder outlet and frozen at –20°C for microbiological and physico-chemical analysis. Additionally, at the 20th day of OOWW1 biotreatment, before starting WW bioreactor feeding, samples of formed biofilms were collected from different bioreactor locations: one sample collected from each quadrant of the column inner wall (BTCI, BTCII, BTCIII, and BTCIV), one in the recirculation pump (BB) and three samples inside the degassing tank (bottom–BFP; middle–BD and top–BTP).

On-line and off-line biotreatment physico-chemical monitoring

Temperature, pH (Ingold), dissolved oxygen (%pO_2; Ingold) and NO_3 (Mettler-Toledo) were on-line monitored using sensors installed in the JLR during the experiment. Off-line measurement of COD was performed in samples taken from the reactor according with standard methods (American Public Health Association 1998). Off-line determination of ammonia (NH_4) was done using a selective probe (Crison) following manufacturer's instructions.

DNA extraction

A volume of 50 ml wastewater aliquots were centrifuged at 12,900*g* for 20 min to obtain total genomic DNA from samples collected during JLR biotreatment. Pellets were mixed with 10 ml of DNA extraction buffer containing 1% CTAB (hexadecylmethylammonium bromide) according to Zhou et al. (1996) with modifications as follows: supernatants obtained from the extraction step were combined and mixed with an equal volume of chloroform:isoamyl alcohol (24:1, vol/vol). The aqueous phase was recovered by centrifugation, and

0.1 volume of 3 M sodium acetate was added before precipitation with 0.6 volume of isopropanol.

PCR amplification for TGGE analysis

For TGGE analysis, approximately 200 base pairs (bp) of the 5′ end of the V3 variable region of bacterial 16S rRNA genes were amplified with Eubacteria-specific primers 341F-GC (5′-CCT ACG GGA GGC AGC AG-3′) and 534R (5′-ATT ACC GCG GCT GCT GG-3′) (Muyzer et al. 1993). The primer F341-GC contained at its 5′ end a 40-base GC-clamp (5′-CGC CCG CCG CGC GCG GCG GGC GGG GCG GGG GCA CGG GGG G-3′) to stabilize the melting behaviour of the DNA fragments (Muyzer et al. 1993). The PCR mixture contained (50 µl final volume with sterile water): 5 µl of 10× PCR buffer (Invitrogen, Belgium), 2 µl of 50 mM $MgCl_2$ (Invitrogen, Belgium), 1 µl of 10 mM dNTP mixture (Invitrogen, Belgium), 1 µl of a 50-pmol/µl of each primer (Invitrogen, Belgium), 0.2 µl of *Taq* polymerase (5 U/µl; Invitrogen, Belgium), 2.5 µl of BSA 0.1%, and 1 µl of the extracted DNA. Appropriate negative (without DNA) and positive (with *E. coli* genomic DNA) controls were included. PCR reactions were performed in thermocyclers (BIOMETRA) as follows: an initial 5 min denaturation at 94°C was followed by 35 cycles of denaturation at 94°C for 60 s, annealing at 55°C for 60 s and elongation at 72°C for 60 s, and a final 5 min chain elongation at 72°C. All the PCR products were separated on 1% (w/v) agarose gels in 0.5× TAE buffer, at 100 V for 1 h, using the 1 kb plus DNA Ladder (Gibco-BRL) as molecular size marker. After staining with ethidium bromide (5 mg l^{-1}), the image obtained under u.v. light was digitized using the Kodak 1D 2.0 Analysis Software (Rochester, New York, USA).

16S-TGGE analysis

For parallel TGGE analysis, re-amplified PCR products with primers 341F-GC/534R were electrophoresed using a TGGE Maxi system (Biometra, USA) according to the manufacturer's instructions. Aliquots of each PCR mixtures (100–300 ng/sample) were applied in a gel containing 6% (w/v) acrylamide/bisacrylamide (39:1), 8 M urea, 2% (v/v) glycerol and 20% (v/v) formamide in 1× TAE buffer system, at a constant voltage of 150 V, for 20 h, applying a temperature gradient of 44–52°C (0.47°C/cm gel). Before electrophoresis, the gel was equilibrated to the temperature gradient for 20 min. After the completion of electrophoresis, the gel was silver stained and photographed using a digital camera and scanned.

Preparation of a TGGE temperature-reference marker

In order to allow gel-to-gel comparisons, a TGGE temperature-reference marker containing a mixture of 16S rRNA gene fragments amplified with primers 341F-GC and 534R was prepared. Denaturation kinetics of these amplified 16S rRNA gene fragments influence their migration in the gel allowing its correlation with the selected temperature gradient, since a GC-clamp was added to the forward primer during amplification reaction. This procedure allows normalization of gels taking into account for probable temperature degree deviation along the gel. Aliquots (5 µl) of the TGGE temperature-reference marker containing the amplified mixture (20–30 ng/sample) were electrophoresed in the gel containing 6% (w/v) acrylamide/bisacrylamide (39:1), 8 M urea, 2% (v/v) glycerol and 20% (v/v) formamide in 1× TAE buffer. Electrophoresis was performed at constant voltage of 120 V, for 20 h, with a temperature gradient of 44 up to 52°C (0.47°C/cm gel). Before electrophoresis, the gel was equilibrated to the temperature gradient for 20 min. After the completion of electrophoresis, the gel was silver stained and photographed using a digital camera and scanned.

The TGGE temperature-reference marker was prepared from seven different bacterial strains: I—*Aerococcus* sp. CS052 (BioFIG—Centre for Biodiversity, Functional, and Integrative Genomics, Portugal), II—*Lactobacillus brevis* CECT 4390 (CECT—Colección Española de Cultivos Tipo, Spain), III—*Acinetobacter* sp. CS041 (BioFIG), IV—*Streptococcus* sp. CS005 (BioFIG), V—*Campylobacter fetus* DSM 5361 (DSM—Deutsch Sammlung von Mikroorganismen, German), VI—*Azospirillum* sp. MGCA283 (BioFIG), VII—*Acetobacter aceti* CECT 298 (CECT). The roman numbers indicate the order from top to bottom in the TGGE band pattern (Fig. 1).

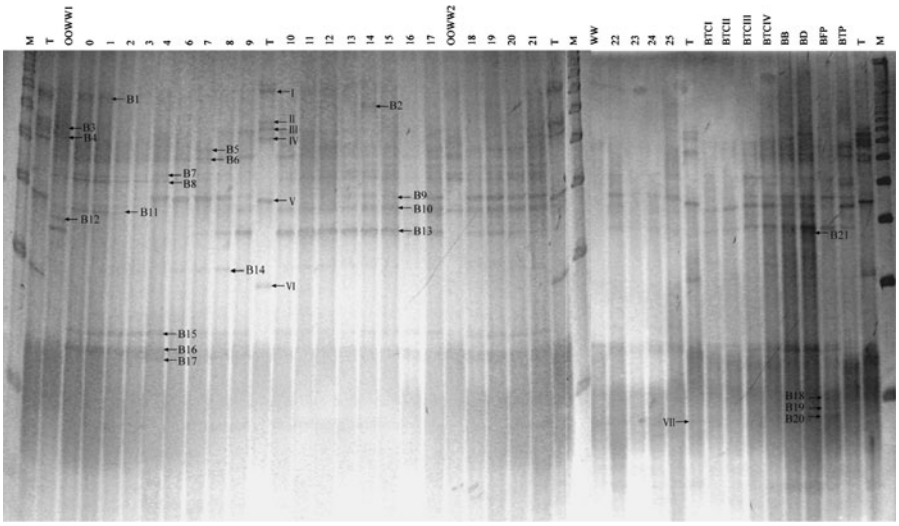

Fig. 1 TGGE band profiles of V3 fragments of 16S rDNA gene amplified with universal primers 341F-GC and 534R. *Lanes* represent samples taken during JLR biotreatment (0 up to 25), and collected from wastewaters (OOWW1, OOWW2 and WW) and from biofilms (BTCI, BTCII, BTCIII, BTCIV, BB, BD, BFP and BTP). *Arrowheads* indicate excised bands which correspond to clones B1 to B21, and the bands corresponding to the bacterial strains prepared for temperature-reference marker I–VII (as described in Material in Methods section). *M* DNA 100 bp ladder plus marker, *T* TGGE temperature-reference marker

Cloning, sequencing and phylogenetic affiliation of TGGE bands

Selected bands were excised from TGGE gels with a sterile scalpel, re-suspended in 50 µl of sterile Tris–EDTA buffer, and stored at 4°C overnight. Elute was subjected to PCR of V3 fragments using primers 341F-GC and 534R under the same conditions as described above. However, 4 µl of eluted DNA fragments were added to the 50 µl PCR mixture. The PCR products were purified using the Jet Quick PCR Purification Spin Kit/250 (Genomed), according to the manufacturer's instructions.

Purified PCR products were visualized by electrophoresis on 1% agarose gel, at 100 V for 1 h, and were cloned in *E. coli* XL1-Blue MRF' (Stratagene) by using the pCR II (Invitrogen) vector system, following the protocol of the manufacturer. Preparation of competent *E. coli* cells was according to Chung et al. (1989). The ligation product transformed into *E. coli* XL1-Blue allows a blue/white colonies screening on medium Luria–Bertani (LB) containing ampicillin (100 µg ml^{-1}), tetracycline (12.5 µg ml^{-1}), X-Gal (5-bromo-4-chloro-3-indolyl-*b*-D-galactopyranoside, 80 µg ml^{-1}) and IPTG (Isopropyl-*β*-D-thiogalactoside, 80 µg ml^{-1}). Corresponding to each TGGE excised band, three colonies of ampicillin-resistant transformants (white) were randomly selected and transferred with a sterile toothpick to 50 µl of TE containing 0.1% Tween 20 and were boiled for 10 min to lyses the cells. Subsequently, PCR was performed with the vector-specific primers T7 (5′-TAA TAC GAC TCA CTA TAG GG-3′) and SP6 (5′- ATT TAG GTG ACA CTA TAG AAT AC). The PCR mixture contained (50 µl final volume with sterile water): 5 µl of 10× PCR buffer (Invitrogen, Belgium), 2 µl of 50 mM $MgCl_2$ (Invitrogen, Belgium), 1 µl of 10 mM dNTP mixture (Invitrogen, Belgium), 1 µl of a 50-pmol/µl of each primer (Promega), 0.2 µl of *Taq* polymerase (5 U/µl; Invitrogen, Belgium), 2.5 µl of BSA 0.1%, and 4 µl of the cell lysates as the template. PCR reactions were performed in thermocyclers (BIOMETRA) as follows: an initial 5 min denaturation at 94°C was followed by 35 cycles of denaturation at 94°C for 60 s, annealing at 50°C for 60 s and elongation at 72°C for 60 s, and a final 5 min chain elongation at 72°C. All the PCR products were analyzed by electrophoresis, in 1% (w/v) agarose gel and TAE buffer, at 100 V, visualized by ethidium bromide (5 mg l^{-1}) staining under u.v. light and documented using KODAK 1D Image Analysis Software (Rochester, New York, USA).

For sequencing of the cloned PCR fragments, 20 µl of the PCR products generated with primers T7 and SP6 were purified with a Jet Quick PCR Purification Spin Kit/250 (Genomed), according to the manufacturer's instructions, and were sequenced with an automated DNA sequencer (Ceq 2000XL DNA System Analyser, Beckman Coulter). The BLAST tool of the National Center for Biotechnology Information (http://www.ncbi.nlm.nih.gov) was used to find homologous and other close sequences (97–100% identity) for the phylogenetic affiliation of nucleotide sequences obtained from TGGE.

PCR amplification for LH-PCR analysis

For LH-PCR analysis, V1, V2 and V3 regions of bacterial 16S rRNA genes were amplified with Eubacteria-specific primers: fluorescently labelled forward 27F (5′-[6FAM] AGAGTTTGATCCTGGC TCAG-3′) (Massol-Deya et al. 1995) and unlabelled reverse 534R (Muyzer et al. 1993). 27F-FAM was 5′ end labeled with phosphoramidite fluorochrome 5-carboxyfluorescein (5′ 6-FAM). Aliquots (10 ng) of extracted DNA from each sample were used as template for amplification. The PCR mixture is the same as described for TGGE analysis. PCR reactions were performed in thermocyclers (BIOMETRA) as follows: an initial 3 min denaturation at 94°C was followed by 35 cycles of denaturation at 94°C for 45 s, annealing at 55°C for 45 s and elongation at 72°C for 2 min, and a final 5 min chain elongation at 72°C. All the PCR products were analyzed by electrophoresis, in 1% (w/v) agarose gel and TAE buffer, at 100 V, visualized by ethidium bromide (5 mg l^{-1}) staining under u.v. light and documented using KODAK 1D Image Analysis Software (Rochester, New York, USA). LH-PCR products concentrations were estimated against a standard λ DNA solution of different known concentrations by electrophoresis in a 1% agarose gel stained with ethidium bromide (5 mg l^{-1}). Twenty-five nanograms of LH-PCR products were analyzed with an automated DNA sequencer (Ceq 2000XL DNA System Analyser, Beckman Coulter). The software outputs electropherograms, in which peaks with different sizes (in base pairs) represent the bands and the integrated fluorescence of each band is the area under the peaks. The relative abundance of each amplicon was estimated as the ratio between the integrated fluorescence of each of the peaks and the total integrated fluorescence of all peaks. To test the reproducibility of the method, 10% of the total number of the samples was randomly selected as replicates and submitted to LH-PCR analysis at the experimental conditions mentioned above.

Cluster analysis of TGGE and LH-PCR fingerprints

The hierarchical clustering of microbiota from biotreatment, based on their fingerprinting patterns (scanned TGGE gels and LH-PCR electropherograms), was performed using BioNumerics software v4.0 (Applied Maths, Belgium). For TGGE fingerprints, association was calculated with Dice similarity coefficient (Dice 1945), whereas Pearson's correlation coefficient was applied for LH-PCR patterns. The dendrograms were constructed with UPGMA clustering method.

Diversity index calculations

TGGE and LH-PCR fingerprint data were used to evaluate the structural diversity of the microbiota, being these results also useful to compare both molecular tools. The Shannon–Weaver diversity index (H'; Shannon and Weaver 1963) is calculated by using the following equation: $H' = -\sum_{i=1}^{S}(ni/N)ln(ni/N)$, assuming that n_i is the relative intensity (area) of each TGGE band (in the gel) or LH-PCR peak (in the electropherogram), N is the sum of all the intensities (areas) of all TGGE bands or LH-PCR peaks, for each analysed sample, and S is the number of TGGE bands or LH-PCR peaks. The evenness index (E; Pielou 1966) or the equitability of the samples was calculated from the Shannon–Weaver diversity function as follows: $E = H'/lnS$, where S is species richness in the microbiota, i.e., the total number of TGGE bands or LH-PCR peaks. This value tend towards for the minimum value (zero) as a species became dominant in the community, or for the maximum value (1) as the more equitable will be the distribution of individuals for the species (Ludwig and Reynolds 1988).

Canonical correspondence analysis

Canonical correspondence analysis (CCA) was performed using CANOCO for Windows v4.5 software

(Biometris, The Netherlands; ter Braak and Verdonschot 1995) to explore multivariate relationships between environmental parameters (after standardization) and the members of microbiota (TGGE banding profiles), and its significance was assessed by Monte Carlo test using 1,000 permutations. The resulting ordination biplot approximated the weighted average of each species (in this case, bands intensity) with respect to environmental variables (represented by *arrows*). The length of these arrows indicated the relative importance of that environmental factor in explaining variation in bacterial profiles, while the angle between the arrows indicated the degree to which they were correlated.

Community level metabolic profile analysis

All samples collected from biotreatment were 10% diluted to prepare cell suspensions for analysis. Preparation of cell suspensions and the subsequent inoculations were performed according to the user's manual (Biolog, Inc) unless otherwise specified. Metabolic utilization pattern by each microbiota was performed inoculating Biolog EcoPlates (Biolog, Inc) with 150 µl of each microbial inoculum suspended in phosphate buffer. The EcoPlate contains three replicate wells of 31 carbon substrates (Choi and Dobbs 1999) and a control well, with no added carbon substrate. After inoculation, substrate consumption was detected by measuring the absorbance at 595 nm, using a microtiter plate reader (Athos, Zenith 3100), at intervals of 6 and 12 h up to 170 h.

Results and discussion

Microbiota structure and dynamics analysis

To analyse microbiota structure along the biotreatment, molecular profiles were determined using the two fingerprinting methods, TGGE and LH-PCR, for analysis of 16S rRNA gene fragments.

Molecules with different sequences have a different melting behaviour allowing the separation of 16S rRNA gene fragments due to differences in migration in polyacrylamide gel containing a linear temperature gradient. This is the basis of TGGE (Muyzer 1998, 1999; Muyzer and Smalla 1998). The TGGE banding pattern profiles of 16S rRNA gene fragments reamplified with primers 341F-GC e 534R have shown a very good separation and resolution (Fig. 1). High number of bands was observed on TGGE profiles obtained from samples collected at different HRT. In addition, several profiles showed a high number of common bands at the same relative position of the gel with variable relative intensities. This could indicate differences in the relative abundance of some common bacterial species present in the different samples collected along the biotreatment. Most of the dominant bands are present in all analysed samples.

Assuming that bands with same migration correspond to same populations, the selection of bands was based in their intensity and dominance on TGGE profiles, in order to evaluate, respectively, the most abundant populations and the more representative on the biotreatment. However, some of the bands with low frequency and low intensity (e.g. B21) were also selected to evaluate the eventual relevance of the corresponding species. Phylogenetic affiliation from nucleotide sequences was determined from selected bands of TGGE profiles. Bands were excised, reamplified with primers 341F-GC e 534R, cloned, purified and sequenced. A similarity search was performed using the BLAST tool (http://www.ncbi.nlm.nih.gov), and results obtained are shown in Table 1. After sequence analysis, one TGGE band was found to be chimerical and, therefore, it was not considered for this analysis. Twenty-one OTUs were identified and phylogenetically affiliated with typical microorganisms found in this type of effluents. Identified microorganisms were distributed among the five main phylogenetic groups as follows: 40% belonging to alpha-Proteobacteria class, 20% to Firmicutes phylum, 20% to Bacteroidetes phylum, 15% to gamma-Proteobacteria class, and 5% to beta-Proteobacteria class (Table 1). Among the 21 OTUs, 15 were identified as being closely related with known cultivable species, with a similarity of sequences higher than 96%.

As shown in Fig. 2, cluster analysis of TGGE profiles grouped samples in five main clusters (I up to V) with a similarity higher than 79%. Samples from OOWW1 and WW (raw effluents) were not directly grouped with any sample collected during the biotreatment. Cluster I, with a similarity coefficient of 79%, is composed by two samples collected at batch phase of the biotreatment and one sample from HRT 6 days. Cluster II, with a similarity coefficient

Table 1 Phylogenetic affiliations of the 21 nucleotide sequences obtained from bands excised from TGGE profiles

Clone	Similar organism	Access code	Similarity (%)	Phylogenetic affiliation
B07	*Sphingomonas wittichii* RW1, complete genome	CP000699	100	Alpha-proteobacteria
B09	Uncultured *Sphingomonas* sp. clone U000130465 16S rRNA gene, partial sequence	FJ037510	100	
B11	*Novosphingobium aromaticivorans* 16S rRNA gene, partial sequence	AB331237	98	
B13	*Sphingomonas paucimobilis* 16S rRNA gene, partial sequence	U20776	100	
B14	*Gluconacetobacter diazotrophicus* strain 4L, 16S rRNA gene, partial sequence	DQ387435	98	
B17	*Gluconacetobacter diazotrophicus* PAl 5, complete genome	AM889285	100	
B18	*Sphingobium yanoikuyae* S27, 16S rRNA gene, partial sequence	AY972400	99	
B20	Uncultured *Novosphingobium* sp., 16S rRNA gene, partial sequence	EU670667	98	
B21	Clone of alpha proteobacterium AKYG623, 16S rRNA gene, partial sequence	AY922042	100	
B06	*Ralstonia eutropha* 16S rRNA gene, complete sequence	AF027407	98	Beta-proteobacteria
B02	*Pseudomonas* sp. BSs20166, 16S rRNA gene, partial sequence	EU365518	99	Gamma-proteobacteria
B04	*Pseudomonas* sp. SMCC B0138, 16S rRNA gene, partial sequence	AF500276	98	
B12	*Klebsiella* sp. HPC70, 16S rRNA gene, partial sequence	AY996984	100	
B01	*Lactobacillus vaccinostercus,* 16S rRNA gene, partial sequence (ATCC 33310 = JCM 1716)	AB362703	97	Firmicutes
B03	*Lactobacillus plantarum* strain IMAU60026, 16S rRNA gene, partial sequence	FJ211392	97	
B05	*Lactobacillus manihotivorans* strain OND 32, 16S rRNA gene, complete sequence	AF000162	100	
B16	*Lactobacillus* sp. NS123, 16S rRNA gene, partial sequence	EU177637	96	
B08	Uncultured *Prevotella* sp. clone J28, 16S rRNA gene, partial sequence	DQ168844	95	
B10				
B19				Bacteroidetes
B15	*Sphingobacterium*-like sp. PC1.9, partial 16S rRNA gene	X89912	97	

of 83%, involves four samples taken at a HRT 6 days, the sample from OOWW2, and the sample 21 collected at HRT 4.5 days. Samples that achieved good COD removal rates (58–71%) constitute this cluster. Phylotypes most closely related to *Gluconacetobacter diazotrophicus, Lactobacillus* spp., *Novosphingobium* sp., *Pseudomonas* sp., *Ralstonia eutropha, Sphingobacterium*-like sp., and *Sphingomonas paucimobilis* are dominant in the corresponding microbiota. Cluster III, with a similarity coefficient of 86%, grouped all the samples collected during the continuous regimen reactor at HRT 4.5 days (excluding sample 21). A sample taken at day 0 (batch phase) and three samples collected under HRT 6 days (at the 7th, 13th and 17th days of biotreatment) also grouped in this cluster. The microbiota found in this cluster is mainly dominated by phylotypes most closely related to *Lactobacillus manihotivorans*, *Lactobacillus* spp., *Novosphingobium aromaticivorans*, *Prevotella* sp., *Ralstonia eutropha, Sphingobacterium*-like sp. and *Sphingomonas wittichii*. It should be emphasized that this cluster stands out since grouped the highest number of samples including six of them with high values of COD removal rates (65–75%). All the biofilm samples grouped with the two samples taken at the final phase of the biotreatment (24th and 25th day) in cluster IV, with a similarity coefficient of 87%. *Lactobacillus plantarum*, *Klebsiella* sp. and the phylotype related to uncultured alpha proteobacterium were only found in the biofilms composition. The main differences found between biofilms microbiota are that besides the other common populations, *Gluconacetobacter diazotrophicus* and *Klebsiella*

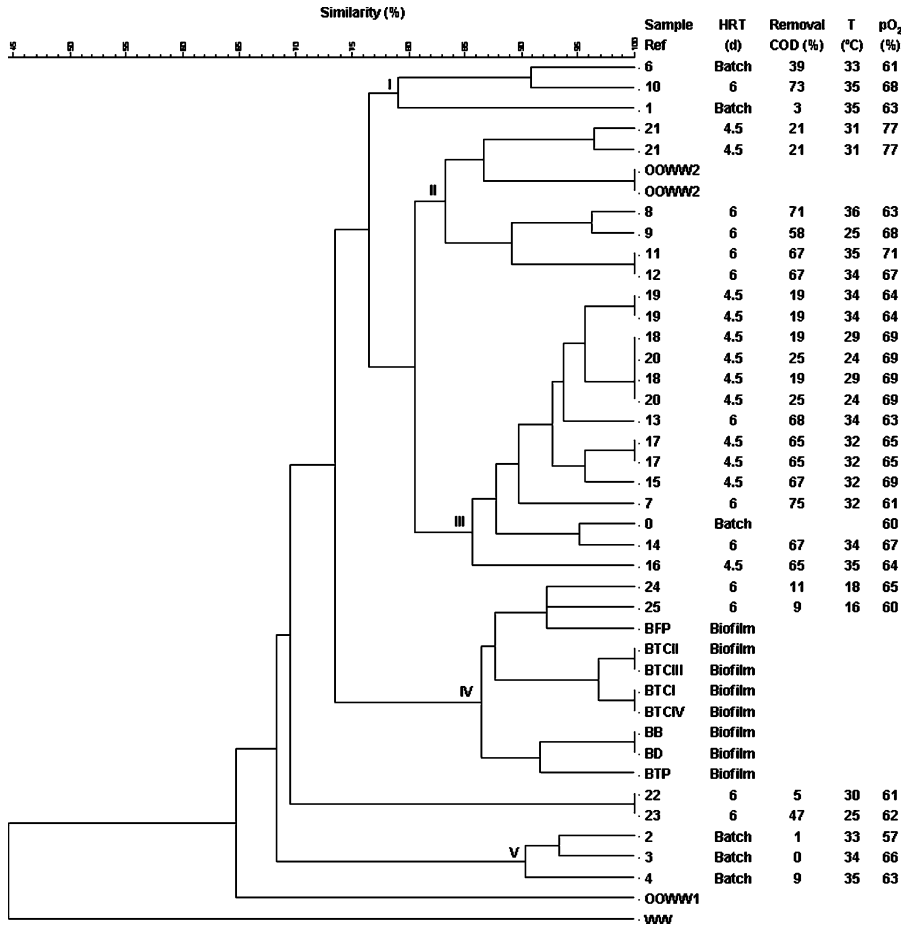

Fig. 2 Cluster analysis of microbiota based on 16S rRNA gene TGGE banding patterns after normalization. Similarity matrices were calculated with the DICE coefficient and dendrogram was generated using the UPGMA method. Samples 17 up to 21 and OOWW2 were run and analyzed in duplicate to test reproducibility of TGGE conditions

sp. are only present in the column inner wall quadrants of the reactor and *Lactobacillus manihotivorans* and *Sphingomonas* sp. were only identified in samples from the recirculation pump and inside the degassing tank., *Pseudomonas* sp. populations that dominated cluster II were detected in the community of microbiota biofilms. The microbiota composition of samples 24 and 25 is the same and quite different from the microbiota from biofilms, given that *Lactobacillus vaccinostercus, Novosphingobium* sp., *Novosphingobium aromaticivorans, Sphingobium yanoikuyae* and *Sphingomonas wittichii* populations were only identified in those samples. Cluster V, with a similarity coefficient of 91%, assembles three samples collected at the start up of the biotreatment (batch phase), and corresponding to the lowest COD removal rates (1–9%). Populations mostly related with *Lactobacillus* sp., *Novosphingobium* sp., *Prevotella* sp., *Ralstonia eutropha*, *Sphingobacterium*-like sp., *Sphingobium yanoikuyae* and *Sphingomonas wittichii* characterize microbiota of this cluster.

The predominance of Gram-negative microbial populations was constant during all the biotreatment including all biofilm samples.

In conclusion, from TGGE band patterns analysis, it could be observed a few effects on the microbiota structure along the biotreatment due to the imposed environmental conditions tested. However, most of the phylogenetic groups identified in the microbiota were detected under all the tested environmental conditions with emphasis to *Lactobacillus* spp., *Ralstonia eutropha* and *Sphingobacterium*-like sp. populations. The strongest alteration in microbiota structure was observed after WW addition with the apparent absence of *Prevotella* sp. and *Pseudomonas* sp. populations. In spite of the dominance by alpha-Proteobacteria detected in the microbiota composition, the presence of phylotypes affiliated with

Pseudomonas sp. and *Lactobacillus manihotivorans*, detected only in clusters II and III, suggests that they were involved in removing organic compounds playing a main role in COD removal rates.

From TGGE cluster analysis, the main shifts in the microbiota structure could be correlated with changes in organic loading charges and simultaneous hydraulic conditions (HRT), thus reflecting the imposed environmental conditions. Resident JLR microbial populations evidence high ability to adapt to environmental conditions shifts, a major factor that directly influences bioreactor efficiency and the ultimate treatment. Although most of the research work on OOWW biotreatment in bioreactors have been carried out in anaerobic conditions, quite a few authors (e.g. Mechichi and Sayadi 2005; Rincón et al. 2006, 2008; Rizzi et al. 2006) referred the existence of important changes within the microbial communities because of increasing organic loading rates or changing HRT. This was attributed to toxicity of the high concentration of OOWW or to the antibacterial activity effect by phenolic compounds that limit microbial activity in biodegradation. On the other hand, the high affinity of some microbial populations for specific organic compounds could favor them even when these substrates are in relative lower concentrations. According to Tiirola et al. (2003), decreasing HRT will increase the selective pressure for high growth rates and shifts in the community structure could be detected.

Bearing in mind that bioreactor performance is strongly dependent upon microbiota ability to adapt to environmental conditions changes (e.g. physico-chemical; hydraulics) which influence the microbiota metabolic activity, TGGE banding patterns were correlated with the tested environmental parameters (temperature, NH_4, NO_3, COD, dissolved oxygen, pH and HRT) by CCA. The sum of all unconstrained eigenvalues indicated an overall variance in the dataset of 0.314 (data not shown). Total variation that could be explained by environmental variation accounted for 0.351, as indicated by the sum of all canonical eigenvalues. Biplot scaling of CCA is shown in Fig. 3. Species–environment correlations were high, especially for axes 1 and 2 (0.886 and 0.830), indicating a relationship between species and environmental variables. The first two axes explained 29.9% of the total cumulative species variance and accounted for 66.1% of the cumulative variance of

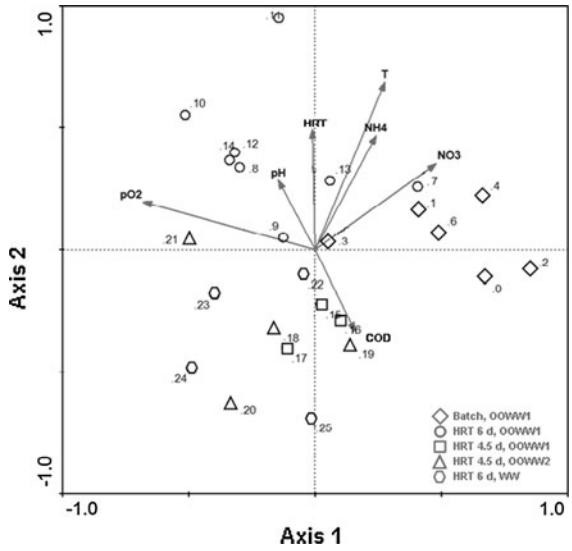

Fig. 3 CCA of biological variables named by 1 up to 25 (TGGE band profiles) and environmental variables signalled by *arrows* (*T* temperature, NH_4, NO_3, *COD* dissolved oxygen, pO_2, pH, HRT)

the species–environment relation whereas all four axes explained 89.4% of the variation ($P < 0.005$). The first ordination axis was mainly correlated to pO_2 level (–0.68), and described a 19.2% of the total variability of the TGGE profiles, while the second ordination axis, which was strongly associated with temperature (0.70), explain 10.7% of the variability. The influence of variation at HRT observed by cluster analysis in the microbiota structure was also confirmed by CCA since this parameter was correlated with the second axis (0.50). Furthermore, the parameters NO_3 concentration correlated with first axis (0.50), and NH_4 concentration correlated with second axis (0.50), were found to be related to shifts of the microbiota structure along the biotreatment. The remaining parameters pH and COD were the most weakly correlated with both first and second axis, indicating their low influence on the microbiota composition and dynamics.

For LH-PCR analysis, V1, V2 and V3 regions of bacterial 16S rRNA genes were amplified with fluorescently labelled forward 27F and unlabelled reverse 534R primers and LH-PCR products were analyzed by capillary gel electrophoresis. The analysis of the dendrogram generated from electropherograms (Fig. 4) revealed five clusters: cluster I grouping 16 samples, with a similarity coefficient

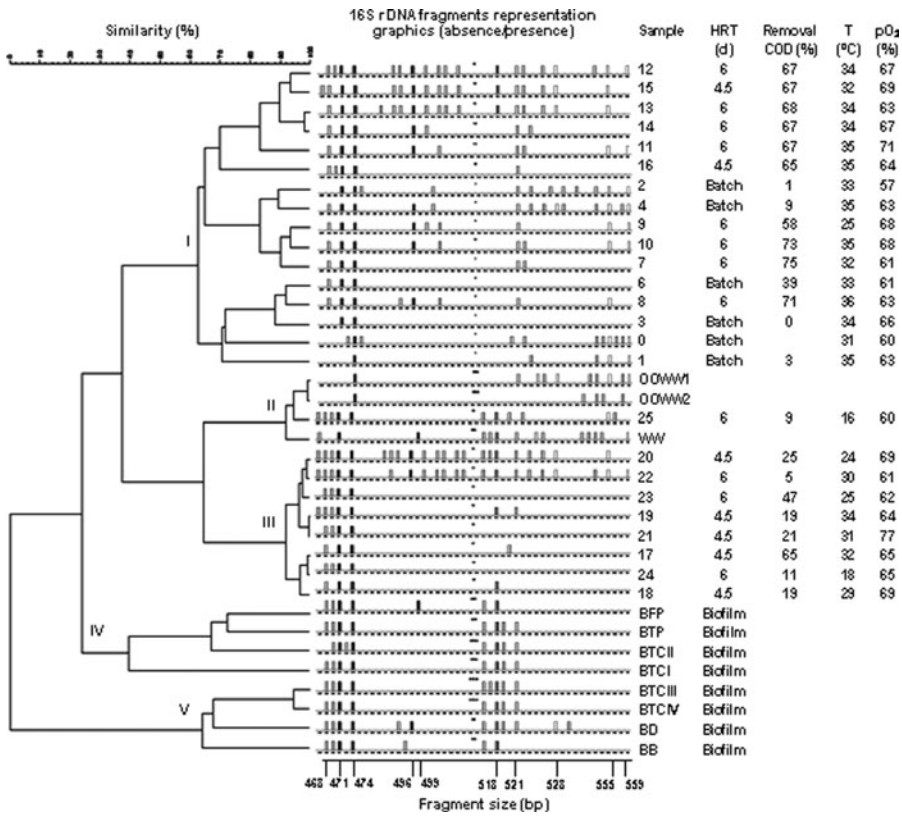

Fig. 4 Cluster analysis of LH-PCR profiles. Similarity matrices were calculated with the Person's correlation coefficient and dendrogram was generated using the UPGMA method

ranging between 62 and 98%; clusters II and III showing similarity coefficient higher than 90%, constituted by 4 and 8 samples, respectively; cluster IV composed by 4 samples, with similarity coefficient ranging between 40 and 74%; and cluster V that grouped four samples, with similarity coefficient ranging between 68 and 96%. Cluster I encloses samples taken during biotreatment of OOWW1: every at the start-up of reactor operation (batch phase) and at HRT 6 days, plus two samples collected at HRT 4.5 days (15th and 16th days). A higher number of bacterial 16S rRNA gene fragments was found in the composition of the microbiota from samples 2 and 4 (batch phase) and also in samples 12 and 15 corresponding to the change of the loading charge of HRT 6 days to HRT 4.5 days. Cluster II grouped the sample collected at the end of the biotreatment (25th day) and samples of the three raw effluents. All the remaining samples were included in cluster III. Biofilm samples were enclosed in clusters IV and V.

Assuming that fragment lengths may be unique to a given taxon as referred by Ritchie et al. (2000), LH-PCR data was also used as an indication of the microbiota composition and structure. This analysis distinguished 21 partial 16S rRNA gene fragments and revealed that its sequence length varied between 468 and 559 bp (Fig. 4). Eight of these fragments (468, 471, 474, 496, 499, 521, 524 and 555 bp) were constantly present in samples collected during the bioreactor feeding at HRT 6 days and coincident with the highest COD removal rates (ranging between 67 and 75%). The change of HRT to 4.5 days caused a high decrease of COD removal rate to approximately 19%, which can be attributed to a remarkable shift in the microbiota structure and related to a decrease in the number of fragments that were previously detected being the fragments 468, 471, 474 and 521 bp constantly found in these samples. These findings support the hypothesis that microbiota found in samples with highest COD removal rates has a fundamental role in this effluent biotreatment. Five fragments with 471, 474, 552, 555 and 559 bp were mainly found in samples collected during batch phase that corresponds to low COD removal rates of zero up to 39%. At the final phase of the biotreatment (after feeding reactor with WW), low COD removal rates (5

to 47%) were achieved being the LH-PCR fragments 468, 470, 471, 474, 514, 518 and 555 bp dominant in the respective samples. From these LH-PCR global data, it can be inferred that COD removal efficiency can be correlated to a determined community structure, represented by specific LH-PCR fragments, but not with the highest diversity of microbiota.

Concerning the structure of the biofilms microbiota and in spite of being collected from different bioreactor sites, it was found high similarity between them and eight LH-PCR fragments (468, 470, 471, 474, 514, 518, 519 and 521 bp) were found to be predominant in all the samples.

Microbiota relative abundance analysis

Table 2 shows the relative abundance profiles obtained with LH-PCR analysis. The relative abundance of each amplified bacterial 16S rRNA gene fragment was estimated as the ratio between the integrated fluorescence of each of the peaks and the total integrated fluorescence of all peaks. In spite of its good reproducibility, peaks heights can only be used as proxies of microbial abundance due to variations in cellular rRNA gene copy number and PCR biases. Although overlapping of fragment size belonging to different bacterial species may occur, in the present study amplicons (i.e., phylotypes) were assumed as isolated 'units' of information for comparison of the generated fingerprinting profiles.

The LH-PCR analysis (Table 2) revealed that short-length PCR products (468, 471 and 474 bp) dominated the biotreatment operation and were detected in all the samples collected from biofilms. More specifically, LH-PCR fragments with 471 and 474 bp have shown the highest relative abundance, accounting for more than 20 and 32% of the calculated total peak area, respectively, in each sample. These results are in agreement with the LH-PCR analysis performed by Tiirola et al. (2003) to characterize bacterial populations present in an inoculum from a full-scale mesophilic activated sludge plant treating wastewaters of integrated pulp and paper mill and bleached kraft mill effluent. As in the studied case of the agro-industrial wastewater biotreatment, short-length PCR products (468–472 bp) dominated the mesophilic-activated sludge accounting for up to 40% of the calculated total peak area. A computer-assisted examination to assign the length variation of fragment sizes in different phylogenetic groups was conducted by Tiirola et al. (2003) and Kolehmainen et al. (2008), based on the cloning and sequencing analysis, suggesting that short rDNA templates (460–478 bp) are derived from members of alpha-proteobacteria. An explanation for the dominance of heterotrophic organisms as alpha-proteobacteria was attributed to the degradation of organic compounds during the wastewater treatment process, what is also in accordance with our results obtained for the molecular characterization of microbiota after phylogenetic affiliation from selected bands of TGGE profiles. The dominance of alpha-proteobacteria was also referred by Pozo et al. (2007) in a TGGE study to characterize the bacterial colonizers of the biofilms formed in submerged aerated filters used for the aerobic treatment of olive washing waters generated in the first steps of olive oil processing.

In what concerns the LH-PCR analysis of crude wastewater samples, these effluents showed a high number of LH-PCR products. The 552 bp fragment with a relative abundance of 69% was the most dominant in OOWW1 and the 555 bp fragment with a relative abundance of 25% was the most dominant in OOWW2. On the other hand, only three LH-PCR gene fragments were detected in WW, being the 474 bp fragment the most dominant with a relative abundance of 68%. It is interesting to note the detection of 519 bp fragment from OOWW2, that was not detected in any sample taken from the biotreatment, but was present in all biofilm samples, being even predominant (more than 40% relative abundance) in biofilms formed on column inner wall quadrants of JLR and in the biofilm taken from the inside of the degassing tank (BTP).

Electropherograms exposed shifts in the microbiota structure and its dynamics along the biotreatment, highlighting the considerable difference among the composition of microbiota characterized in mixed liquor and in the biofilms. However, in spite of shifts in microbial structure resulting from imposed changes in JLR biotreatment conditions, LH-PCR fingerprintings have shown that a great stability of the microbiota composition is observed for each one of the tested hydraulic condition, indicating a rapid microbiota adaptation to changes in environmental conditions inside the bioreactor.

Table 2 LH-PCR analysis of 16S rRNA gene fragments

Relative abundance (%)																				
Fragment length (bp) Sampling	468	470	471	474	492	494	496	498	499	514	518	519	521	524	525	526	528	552	555	557	559
OOWW1	n.d.	n.d.	1.3	n.d.	n.d.	n.d.	1.5	n.d.	n.d.	1.9	11	n.d.	2.2	n.d.	2.0	1.2	n.d.	69	n.d.	n.d.	10
day 0, Batch	n.d.	n.d.	n.d.	18	n.d.	n.d.	n.d.	n.d.	n.d.	n.d.	n.d.	n.d.	n.d.	7.6	n.d.	n.d.	n.d.	12	36	8.2	18
day 1, Batch	n.d.	n.d.	n.d.	57	n.d.	n.d.	n.d.	n.d.	n.d.	n.d.	n.d.	n.d.	n.d.	4.4	n.d.	n.d.	n.d.	7.8	23	n.d.	8.4
day 2, Batch	n.d.	n.d.	21 ± 9	64 ± 12	n.d.	n.d.	n.d.	n.d.	2 ± 1	n.d.	n.d.	n.d.	1 ± 0	n.d.	1 ± 1	n.d.	n.d.	1 ± 0	6 ± 1	n.d.	3 ± 0
day 3, Batch	n.d.	n.d.	13	87	n.d.	n.d.	n.d.	n.d.	nd	n.d.	n.d.	n.d.	n.d.	n.d.	n.d.	n.d.	n.d.	n.d.	n.d.	n.d.	n.d.
day 4, Batch	2.5	n.d.	26	62	n.d.	n.d.	0.6	n.d.	1.3	n.d.	n.d.	n.d.	1.0	0.6	n.d.	0.3	0.9	0.6	2.6	0.3	1.4
day 6, Batch	5.5	n.d.	29	66	n.d.	n.d.	n.d.	n.d.	n.d.	n.d.	n.d.	n.d.	n.d.	n.d.	n.d.	n.d.	n.d.	n.d.	n.d.	n.d.	n.d.
day 7, TRH 6 d	11	n.d.	29	51	n.d.	n.d.	n.d.	n.d.	n.d.	n.d.	n.d.	n.d.	4.2	5.6	n.d.	n.d.	n.d.	n.d.	n.d.	n.d.	n.d.
day 8, TRH 6 d	13	n.d.	35	30	n.d.	2.6	4.3	n.d.	3.4	n.d.	n.d.	n.d.	8.7	n.d.	n.d.	n.d.	n.d.	n.d.	2.4	n.d.	n.d.
day 9, TRH 6 d	6.7	n.d.	33	34	n.d.	n.d.	5.0	2.9	3.8	n.d.	n.d.	n.d.	8.8	n.d.	n.d.	n.d.	n.d.	n.d.	4.0	n.d.	2.3
day 10, TRH 6 d	6.1	n.d.	28	40	n.d.	n.d.	2.6	n.d.	2.6	n.d.	n.d.	n.d.	9.5	3.2	n.d.	n.d.	n.d.	n.d.	4.9	n.d.	2.7
day 11, TRH 6 d	6.3	n.d.	24	39	n.d.	n.d.	3.6	n.d.	3.8	n.d.	n.d.	n.d.	7.7	4.6	n.d.	n.d.	n.d.	n.d.	7.5	n.d.	3.3
day 12, TRH 6 d	5.9	4.0	19	32	1.4	1.2	2.6	1.7	2.3	n.d.	1.3	n.d.	7.9	9.1	n.d.	1.7	3.2	0.6	4.9	n.d.	1.3
day 13, TRH 6 d	12	n.d.	27	32	1.3	1.2	2.4	1.6	1.9	n.d.	1.5	n.d.	6.9	6.9	n.d.	1.7	2.6	n.d.	1.5	n.d.	n.d.
day 14, TRH 6 d	13	n.d.	26	42	n.d.	n.d.	3.8	4.3	n.d.	n.d.	n.d.	n.d.	7.6	3.5	n.d.	n.d.	n.d.	n.d.	n.d.	n.d.	n.d.
day 15, TRH 4.5 d	15	n.d.	25	41	0.8	0.5	1.3	0.8	1.1	n.d.	0.9	n.d.	5.1	3.1	n.d.	1.0	1.7	n.d.	3.5	n.d.	n.d.
day 16, TRH 4.5 d	12	7.0	21	56	n.d.	n.d.	n.d.	n.d.	n.d.	n.d.	n.d.	n.d.	4.4	n.d.	n.d.	n.d.	n.d.	n.d.	n.d.	n.d.	n.d.
day 17, TRH 4.5 d	16	n.d.	23	61	n.d.	n.d.	n.d.	n.d.	n.d.	n.d.	n.d.	n.d.	n.d.	n.d.	n.d.	n.d.	n.d.	n.d.	n.d.	n.d.	n.d.
OOWW2	n.d.	n.d.	n.d.	15 ± 5	n.d.	n.d.	n.d.	n.d.	2 ± 1	n.d.	n.d.	1 ± 1	12 ± 0	n.d.	11 ± 1	5 ± 0	8 ± 0	7 ± 0	25 ± 6	3 ± 1	13 ± 1
day 18, TRH 4.5 d	16	n.d.	21	59	n.d.	n.d.	n.d.	n.d.	n.d.	n.d.	5.1	n.d.	n.d.	n.d.	n.d.	n.d.	n.d.	n.d.	n.d.	n.d.	n.d.
day 19, TRH 4.5 d	14	9.2	19	51	n.d.	n.d.	n.d.	n.d.	n.d.	n.d.	3.8	n.d.	3.1	n.d.	n.d.	n.d.	n.d.	n.d.	n.d.	n.d.	n.d.
day 20, TRH 4.5 d	8.4	8.0	19	42	0.9	1.2	1.4	1.2	1.1	1.1	4.6	n.d.	4.8	2.8	n.d.	0.8	1.4	n.d.	1.4	n.d.	n.d.
day 21, TRH 4.5 d	9.6	9.4	20	61	n.d.	n.d.	n.d.	n.d.	n.d.	n.d.	n.d.	n.d.	n.d.	n.d.	n.d.	n.d.	n.d.	n.d.	n.d.	n.d.	n.d.
WW	n.d.	n.d.	n.d.	68	n.d.	n.d.	n.d.	n.d.	n.d.	n.d.	n.d.	n.d.	n.d.	n.d.	n.d.	n.d.	n.d.	24	n.d.	8	n.d.
day 22, TRH 6 d	11	7.5	26	44	0.6	n.d.	0.8	0.5	1.0	1.0	0.9	n.d.	2.8	1.0	n.d.	0.7	0.7	0.3	1.5	n.d.	0.4
day 23, TRH 6 d	10 ± 1	7 ± 1	29 ± 4	49 ± 10	n.d.	n.d.	0.2 ± 0	n.d.	0.2 ± 0	0.4 ± 0	1 ± 1	n.d.	1 ± 1	n.d.	n.d.	n.d.	n.d.	1 ± 1	1 ± 1	n.d.	n.d.
day 24, TRH 6 d	9.1	9.5	20	62	n.d.	n.d.	n.d.	n.d.	n.d.	n.d.	n.d.	n.d.	n.d.	n.d.	n.d.	n.d.	n.d.	n.d.	n.d.	n.d.	n.d.
day 25, TRH 6 d	11	8.4	24	53	n.d.	n.d.	n.d.	n.d.	n.d.	0.6	0.7	n.d.	n.d.	0.9	n.d.	n.d.	n.d.	n.d.	0.9	n.d.	n.d.
BTC I	2.3	4.9	5.7	19	n.d.	n.d.	n.d.	n.d.	n.d.	13	17	33	5.8	n.d.	n.d.	n.d.	n.d.	n.d.	n.d.	n.d.	n.d.
BTC II	4 ± 3	8 ± 3	7 ± 3	13 ± 1	n.d.	n.d.	1 ± 1	n.d.	n.d.	6.8 ± 2	14 ± 0	41 ± 10	4 ± 0	n.d.	n.d.	n.d.	n.d.	n.d.	n.d.	n.d.	n.d.
BTC III	8.3	12	9.2	8.1	n.d.	n.d.	n.d.	n.d.	n.d.	5.2	10	44	3.4	n.d.	n.d.	n.d.	n.d.	n.d.	n.d.	n.d.	n.d.
BTC IV	6.6	6.8	9.6	12	n.d.	n.d.	n.d.	n.d.	n.d.	8.1	16	35	6.0	n.d.	n.d.	n.d.	n.d.	n.d.	n.d.	n.d.	n.d.

Table 2 continued

Relative abundance (%)																					
Fragment length (bp) Sampling	468	470	471	474	492	494	496	498	499	514	518	519	521	524	525	526	528	552	555	557	559
BB	8.7	9.3	28	37	n.d.	n.d.	n.d.	n.d.	n.d.	4.3	13	n.d.	n.d.	n.d.	n.d.	n.d.	n.d.	n.d.	n.d.	n.d.	n.d.
BD	16	16	27	18	n.d.	2.0	3.0	n.d.	n.d.	3.9	6	2.2	4.3	n.d.	n.d.	n.d.	1.9	n.d.	n.d.	n.d.	n.d.
BFP	11	12	18	41	n.d.	n.d.	3.2	n.d.	n.d.	5.5	10	n.d.	n.d.	n.d.	n.d.	n.d.	n.d.	n.d.	n.d.	n.d.	n.d.
BTP	5.5	4.9	2.6	2.5	n.d.	n.d.	n.d.	n.d.	n.d.	23	16	43	3.5	n.d.	n.d.	n.d.	n.d.	n.d.	n.d.	n.d.	n.d.

Relative abundance of main fragments (percentage of each amplicon area, with a specific length, relatively to total area of peaks) obtained at different hydraulic conditions of wastewaters biotreatment and for all biofilm samples. Samples were randomly selected (OOWW2, 2, 23 and BTCII) to test reproducibility of the method and standard deviation from the average of duplicate reactions is shown

n.d. not detected

Microbiota diversity analysis

The richness and evenness of microbiota reflect selective pressures that figure diversity within communities and the respective measurement of these parameters is most useful while assessing treatment effects on the community diversity. According to Saikaly and Oerther (2004), increasing the diversity of microbiota will increase the possibility for obtaining better-adapted species that will handle specific environmental perturbations. Changing operating parameters of bioreactor could influence the microbial diversity by affecting the nature of competition for essential resources thus being responsible for the dynamic behavior of the microbiota.

Bearing in mind that no single tool allows definitive evaluation of the bacterial diversity, TGGE or LH-PCR fingerprints were used in this study for quick measurement of the diversity and richness of the microbiota for comparative purposes. To determine Shannon–Weaver (H') diversity indices from TGGE or LH-PCR fingerprints, it was assumed that each TGGE band or LH-PCR fragment for each profile could be assign to a specific species (S). In the case of the TGGE band, its intensity is a measure of the number of individuals that belong to that species (n_i) and N is the sum of all the intensities of all TGGE bands. In the case of LH-PCR fragments, the number of individuals that belong to a species (n_i) is considered to be the relative abundance of each amplicon i in proportion to the total area of amplicons in electropherogram (N), for each profile. The LH-PCR and TGGE similarity matrices were used to obtain the diversity indices calculations (Table 3) and high values were achieved for diversity indices and equitability in all samples collected from biotreatment of OOWW1, OOWW2 and WW, including biofilm samples, confirming the diversity of each microbiota. However, these calculations did not clearly reflect that changes in JLR hydraulic conditions are responsible for shifts in microbiota structure. In addition, there are high discrepancies between all diversity indices if calculating from TGGE or LH-PCR fingerprints. Values for richness of species (S), Shannon–Weaver (H') diversity and evenness (E) indices obtained from TGGE fingerprintings were higher and more or less constant during all the biotreatment. Using LH-PCR fingerprintings, the high heterogeneity obtained for

Table 3 Comparison of diversity indices determined from TGGE and LH-PCR fingerprints, for all the samples collected during the biotreatment and all biofilms

Sample	Richness of species (S)[a]		Shannon–Weaver Index (H')[b]		Evenness index (E)[b]	
	TGGE	LH-PCR	TGGE	LH-PCR	TGGE	LH-PCR
OOWW1	12	9	2.38	1.14	0.96	0.52
0	10	6	2.26	1.64	0.98	0.92
1	13	5	2.47	1.20	0.96	0.75
2	8	10	1.98	1.16	0.95	0.50
3	7	2	1.74	0.40	0.89	0.57
4	8	13	1.99	1.17	0.96	0.46
6	10	3	2.18	0.79	0.95	0.72
7	13	5	2.48	1.23	0.97	0.77
8	14	8	2.49	1.65	0.94	0.79
9	13	9	2.45	1.72	0.95	0.78
10	12	9	2.31	1.66	0.93	0.76
11	14	9	2.59	1.78	0.98	0.81
12	14	17	2.53	2.22	0.96	0.79
13	10	14	2.25	1.97	0.98	0.75
14	11	7	2.33	1.55	0.97	0.80
15	11	14	2.33	1.74	0.97	0.66
16	9	5	2.11	1.23	0.96	0.77
17	12	3	2.41	0.93	0.97	0.85
OOWW2	12	11	2.33	2.13	0.94	0.89
18	11	4	2.32	1.08	0.97	0.78
19	12	6	2.41	1.39	0.97	0.77
20	11	16	2.35	1.94	0.98	0.70
21	14	4	2.53	1.07	0.96	0.77
WW	6	3	1.70	0.81	0.95	0.74
22	8	17	1.97	1.69	0.95	0.60
23	8	15	2.03	1.34	0.97	0.50
24	13	4	2.52	1.06	0.98	0.76
25	13	8	2.53	1.28	0.99	0.62
BTCI	15	8	2.61	1.80	0.96	0.87
BTCII	16	10	2.64	1.81	0.95	0.79
BTCIII	16	8	2.52	1.74	0.91	0.84
BTCIV	15	8	2.62	1.88	0.97	0.90
BB	12	6	2.37	1.55	0.95	0.87
BD	12	11	2.39	2.02	0.96	0.84
BFP	13	7	2.46	1.67	0.96	0.86
BTP	12	8	2.33	1.60	0.94	0.77

[a] (S) is the total number of TGGE bands or LH-PCR fragments, in each sample

[b] Shannon–Weaver and evenness indices were determined according to Material and methods

diversity and evenness indices along biotreatment indicates that this method was more accurate to assess shifts occurring in microbiota structure.

The two fingerprinting methods, TGGE and LH-PCR, used to characterise the microbiota structure in this study complemented each other. The main advantages of TGGE and LH-PCR tools are that they require small sample sizes and can be performed with many samples simultaneously. Although both methods generally detect the occurrence of a few dominant groups, TGGE showed more bands compared to the number of fragments in LH-PCR, because LH-PCR is based on the differences in the 16S rRNA gene fragment length whereas TGGE

is based on the difference in the nucleotide composition.

Microbiota metabolic profile analysis

The results obtained were quantitatively (number of positives) and qualitatively (area under the curve of substrate degradation) analyzed, as described by Paixão et al. (2003) and Garland and Mills (1991). The first allows the definition of the amount of substrate that must be degraded being considered as a positive result. The second integrates all the parameters of the growth curve and is considered the best estimative of the community behaviour when growing in that substrate. Together, the areas under the curve in each tested substrate represent the physiological profile of the corresponding microbial community. Figure 5a–c correspond to the graphic representation of both analyses made to samples collected from the biotreatment. Both OOWW and WW contain high concentrations of organic matter, mainly unextracted oil, aromatic compounds, such as polyphenols, sugars and pectic substances, and inorganic salts such as potassium, magnesium and phosphate (Laconi et al. 2007; Tsioulpas et al. 2002) making the Biolog EcoPlates (Biolog, Inc.) suitable for this metabolic profile analysis. Substrates were grouped in seven functional groups (polymers, carbon hydrates, phenols, carboxylic acids, phosphate compounds, amines and amino acids).

The analysis of the graphics obtained shows that the use of some compound was only evident after the fourth treatment day (number of positives changes from zero to 14). The number of positives is variable along the remaining treatment time. The minimum number of positives corresponds to sample 14 (11 positive substrates, 35%) and the maximum to the sample 6 (23 positive results, 74%). Communities 6, 7, 8, 9, 11, 19 and 20 showed the higher metabolic diversity, presenting 20–23 positives (65–74%). The number of positives is higher between the 5th and the 11th day of treatment and shows a reduction from 12 to 18 day. It is higher again between 19 and 21 day; finally, it decreases from the 22nd day, and remains constant until the end of the treatment. These changes do not seem to correlate with changes in effluent neither with the hydraulic conditions tested. On the other hand, the compounds that contribute for the number of positives in each sampling time are also variable, indicating that the dynamics of these microbial populations is complex. Considering the analysis of the area under the curve of each substrate for each community, the physiological profiles of the use of these substrates are not homogeneous, even when analyzed by chemical categories. However, carbon hydrates are the compounds more extensively used by the microbiota, followed by the carboxylic acids and phosphate compounds. An interesting aspect is the utilization of the 4-hydroxybenzoic acid (a phenol) in several samples, but not the 2-hydroxybenzoic acid. Furthermore, sample 20 is the only one that presents a visible growth in this last phenolic compound and is able to grow in the amines phenylethylamine and putrescine. Similarly, sample 19 shows a particular metabolism of D-galacturonic acid. These observations reveal the presence of communities with a distinct degrading potential of an applied interest.

Evaluation of microbiota degradative potential

In order to attribute potential metabolic functions to microbiota populations an integrative analysis was carried out by correlating the molecular fingerprinting profiles with metabolic data.

Fingerprinting analysis using both molecular tools, TGGE and LH-PCR, revealed a clear dominance of alpha-proteobacteria populations along the biotreatment, which were further identified by TGGE analysis to be constituted by microorganisms belonging to genera *Gluconacetobacter, Novosphingobium*, *Sphingobium* and *Sphingomonas*. From TGGE cluster analysis, it was also possible to deduct a microbiota composition with high degradative potential for COD removal, which includes the referred dominant populations plus *Ralstonia eutropha, Lactobacillus* spp., *Prevotella* sp., and *Sphingobacterium*-like sp. populations. Furthermore, also degradative potential for phenol removal could be assigned to this microbiota since utilization of the phenol compound 4-hidroxybenzoic acid was obtained in the metabolic phenol profile analysis.

On the grounds of other published studies, it was possible to assess the functional role of the populations and/or sub-populations identified in the microbiota composition and structure characterized along the biotreatment, aiming to evaluate its potential

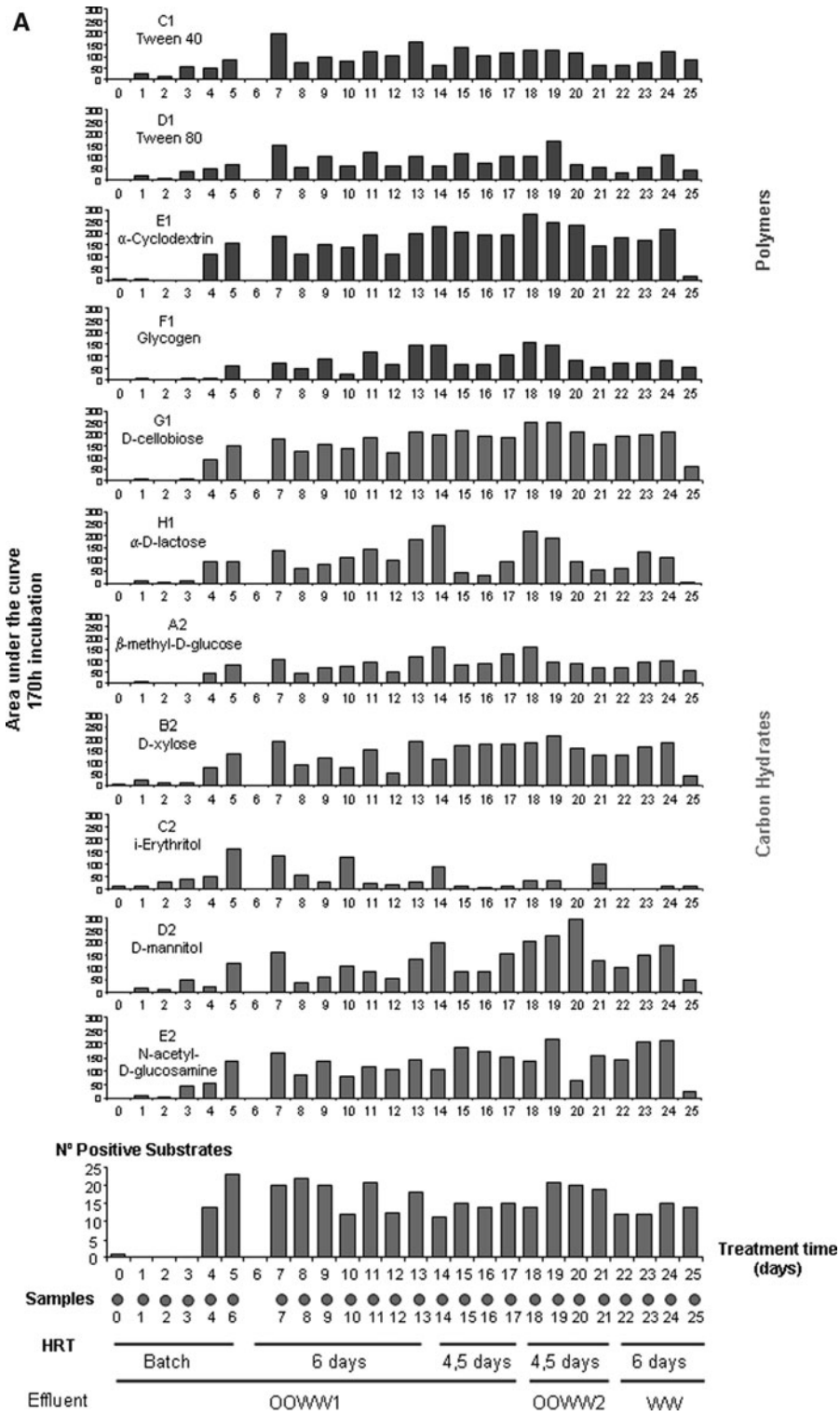

Fig. 5 a–c Graphic representation of quantitative (area under curve of substrate consumption) and qualitative (number of positives) analysis of metabolic activity along biotreatment time. *Circles* mark points corresponding to days of sample collection

Fig. 5 continued

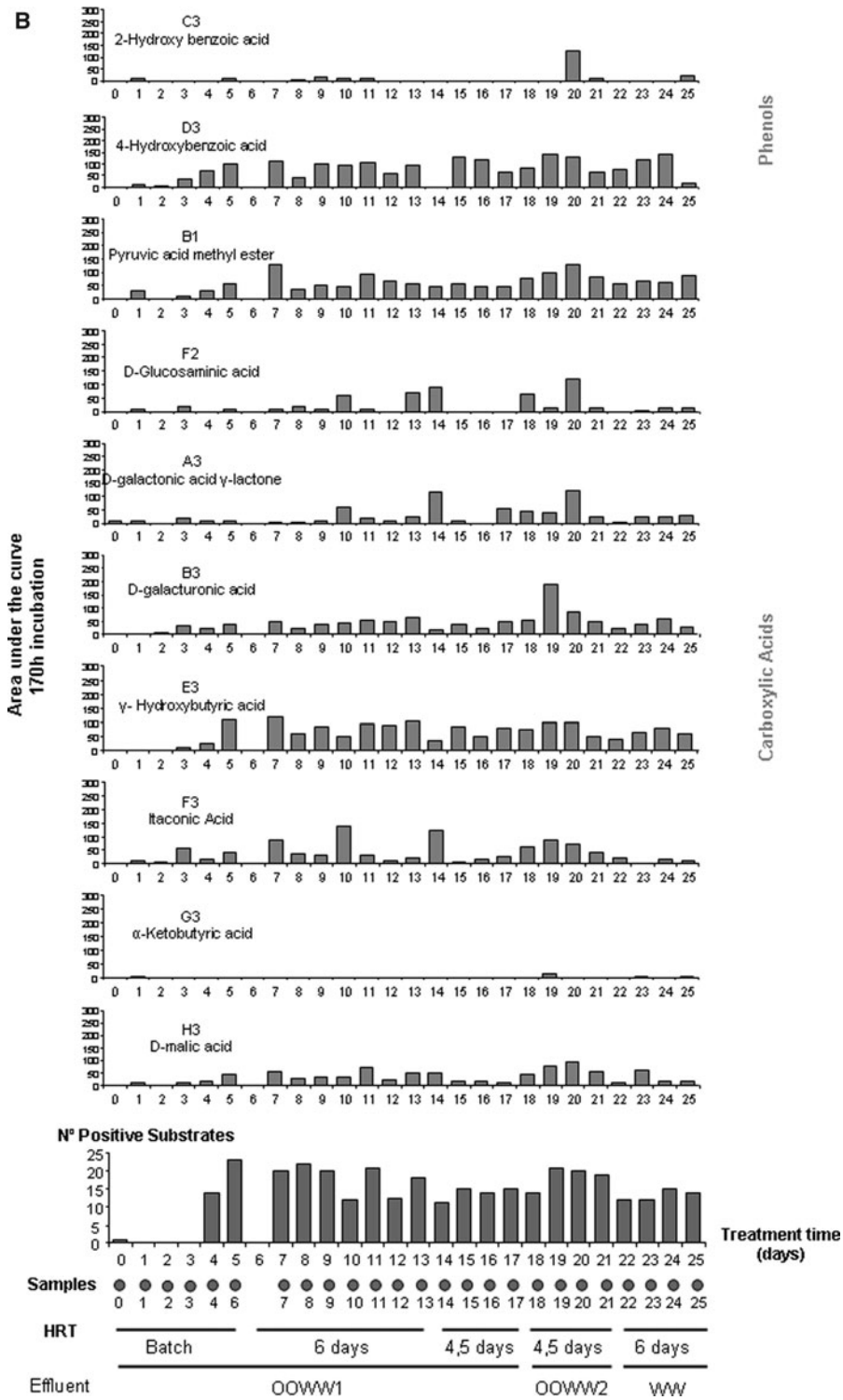

applications and/or to design tailor-made inocula to apply in agro-industrial effluents biotreatments or other applications.

The group Sphingomonadaceae have been utilized in many biotechnological applications, namely in soil bioremediation and polycyclic aromatic

Fig. 5 continued

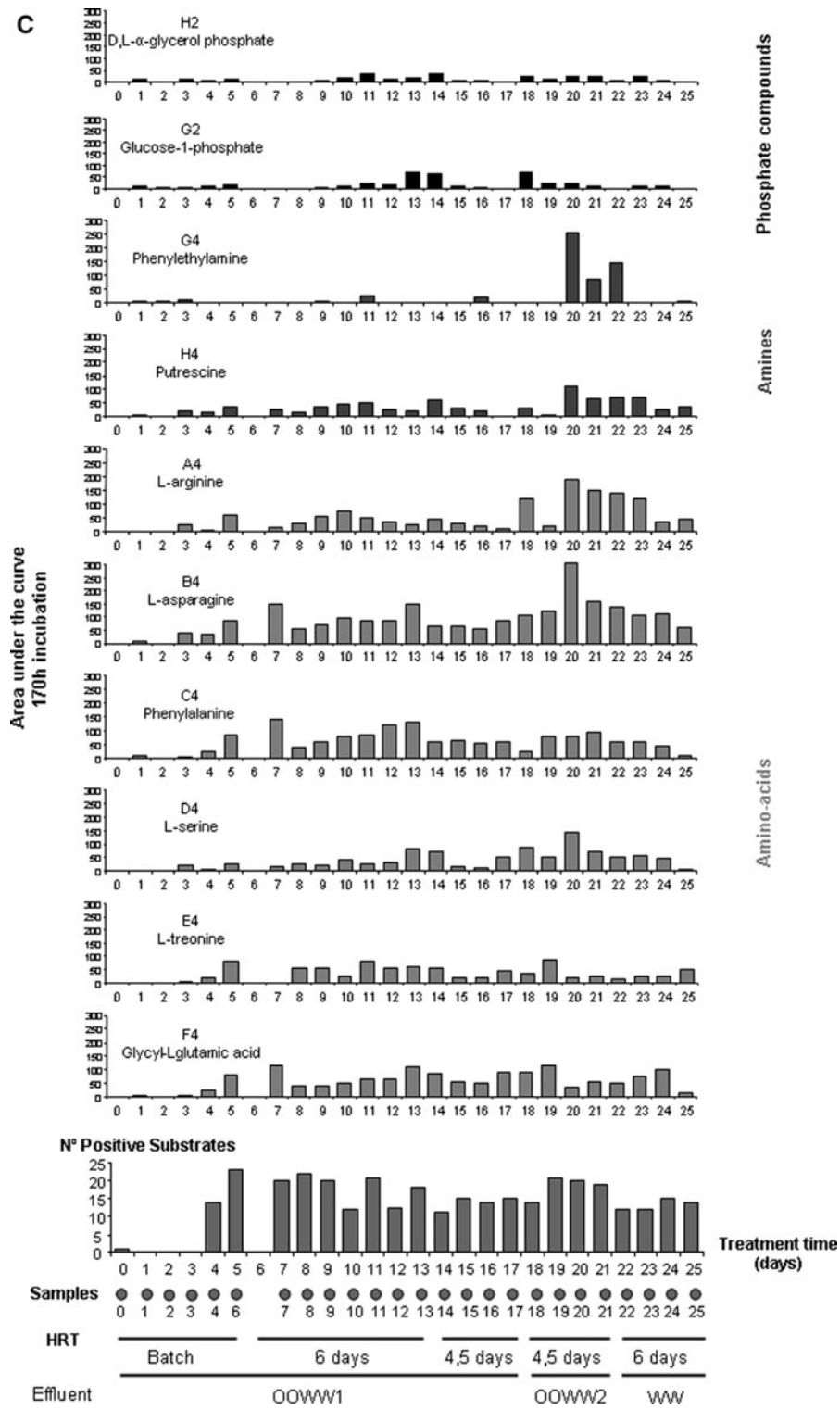

hydrocarbons degradations (Cunliffe and Kertesz 2006) due to their biodegradative and biosynthetic abilities (Stolz 2009). *Sphingomonas* species are very common in terrestrial and aquatic ecosystems, being referred for their ability to metabolize recalcitrant compounds as (poli-) aromatic (halogenated) compounds, dioxins, and several herbicides and pesticides (Baboshin et al. 2008; Böltner et al. 2005; Desai et al. 2008; White et al. 1996). Co-metabolism of anthracene, fluorene and fluoranthene was achieved by a strain of *Sphingomonas* sp. (Zhong et al. 2007). Moreover, strains of genera *Sphingobium* and *Novosphingobium* are known to degrade aromatic and phenolic compounds (Ito et al. 2007; Liu et al. 2005; Tiirola et al. 2002). *Ralstonia eutropha* is often used as a model to study bacterial degradation of aromatic compounds and the sequence of the complete genome is already available for a strain able to degrade 3-chlorobenzoic and 2,4-dichlorofenoxiacetic acids (Trefault et al. 2004). Besides those genera directly correlated with phenolic compound degradation, the presence of *Gluconacetobacter diazotrophicus* in the dominant microbiota could be related with its role in the microbial nitrogen cycle as a nitrogen-fixing organism (Sevilla et al. 2001).

Although *Pseudomonas* sp. populations were not found to be predominant along the biotreatment, Pseudomonadaceae is a group with important environmental functions, e.g. plant growth promoters, and bioremediation of toxic residues (Nelson et al. 2002; Tombolini et al. 1997; Wang et al. 2008) as well as xenobiotic compounds degradation (Timmis 2002). Dominance of strains of *Pseudomonas* sp. have also been reported in phenols degradation during effluents biotreatments processes (El Fantroussi and Agathos 2005; Watanabe et al. 1998, 2002; Whiteley et al. 2001), and in habitats polluted with 2,4,6-trinitrotoluene (George et al. 2008). In addition, it should be emphasized that *Pseudomonas* and *Ralstonia* strains when combined in a co-culture, complemented each other with respect to their ability to degrade monoaromatic compounds present in OOWW (Di Gioia et al. 2001).

Comparing the microbiota composition of biofilms with mixed liquor samples, the major difference observed is the absence of *Lactobacillus plantarum* and *Klebsiella* sp. in the samples collected along the biotreatment. This fact may be ascribed to their ability to form aggregates and biofilms in a wide range of different environments as an important colonization strategy, highlighting the preponderant and dual role of surface exopolysaccharides, which either mask potential bacterial surface structures or rather promote biofilm maturation (Balestrino et al. 2008; Ude et al. 2006). The detection of *L. plantarum* in biofilms could be associated to the fact that its growth rather occurs at conditions with low redox potential and low oxygen content, which may be formed inside the biofilms. The capacity to decrease the redox potential and to promote the inverse reaction of auto-oxidation of phenolic compounds to tannins present in OOWW, by reductive depolymerisation of polyphenols, leads to decolourization and biodegradation of these compounds (Ayed and Hamdi 2003). Based on the capacity to degrade 97% of gallic acid, a *L. plantarum* strain was selected by Guzmán-López et al. (2009) for further studies about the effect of phenolic compounds in growth of lactic acid bacteria.

Conclusions

Determination of the microbiota structure by TGGE analysis showed the dominance of alpha-proteobacteria group during the aerobic biotreatment of OOWW in a JLR. Phylotypes affiliated with *Lactobacillus* spp., *Ralstonia eutropha* and *Sphingobacterium*-like sp. were detected under all the environmental conditions tested but the main role in COD removal rates was assigned to the phylotypes affiliated with *Pseudomonas* sp. and *Lactobacillus manihotivorans*. Temperature and oxygen level fluctuations were the main responsible parameters for the microbiota dynamics along the biotreatment, and a minor influence was due to NO_3, NH_4 and HRT variations. Moreover, through LH-PCR analysis, association was found between eight 16S rRNA gene fragments and the samples showing the highest biotreatment performance. The analysis of microbiota relative abundance by LH-PCR revealed that three short-length PCR products dominated the biotreatment operation being also detected in all the samples collected from biofilms. Cluster analysis of both TGGE and LH-PCR fingerprinting profiles revealed that the shifts observed in the microbiota structure seemed to be dependent upon tested changes in HRT. The data obtained from phylogenetic and metabolic

profile analysis allowed to infer a microbiota with high degradative potential for COD removal and aromatic compounds. This approach could be useful for the development of novel shaped inocula with specific metabolic function for effluents biotreatment technologies and/or other biotechnological applications. Additionally, construction of metagenomic libraries based on collected samples from these biotreatments is a promising via to study new aspects of microbiological activity of these complex and different microbiota, as well as to identify new species, genes and/or metabolites.

Acknowledgments This work was supported by the FCT Project MOTIVE (PPCDT/AMB/56616/2004). Sandra Chaves was a FCT post-doc fellow (BPD/20819/2004). Authors wish to thank José Cardoso Duarte from LNEG (Unidade de Bioenergia) for jet-loop reactor availability.

References

American Public Health Association (1998) Standard methods for the examination of water and wastewater, 20th edn. American Public Health Association, Washington, DC, USA

Ayed L, Hamdi M (2003) Fermentative decolorization of olive mill wastewater by *Lactobacillus plantarum*. Process Biochem 39:59–65. doi:10.1016/S0032-9592(02)00314-X

Baboshin M, Akimov V, Baskunov B, Born TL, Khan SU, Golovleva L (2008) Conversion of polycyclic aromatic hydrocarbons by *Sphingomonas* sp. VKM B-2434. Biodegradation 19:567–576. doi:10.1007/s10532-007-9162-2

Balestrino D, Ghigo J-M, Charbonnel N, Haagensen JAJ, Forestier C (2008) The characterization of functions involved in the establishment and maturation of *Klebsiella pneumoniae* in vitro biofilm reveals dual roles for surface exopolysaccharides. Environ Microbiol 10(3):685–701. doi:10.1111/j.1462-2920.2007.01491.x

Bernhard AE, Colbert D, McManus J, Field KG (2005) Microbial community dynamics based on 16S rRNA gene profiles in a Pacific Northwest estuary and its tributaries. FEMS Microbiol Ecol 52:115–128. doi:10.1016/j.femsec.2004.10.016

Böltner D, Moreno-Morillas S, Ramos J-L (2005) 16S rDNA phylogeny and distribution of *lin* genes in novel hexachlorocyclohexane-degrading *Sphingomonas* strains. Environ Microbiol 7(9):1329–1338. doi:10.1111/j.1462-2920.2005.00820.x

Borja R, Rincón B, Raposo F, Alba J, Martín A (2002) A study of anaerobic digestibility of two-phases olive mill solid waste (OMSW) at mesophilic temperature. Process Biochem 38:733–742. doi:10.1016/S0032-9592(02)00202-9

Choi KH, Dobbs FC (1999) Comparison of two kinds of biolog microplates (GN and ECO) in their ability to distinguish among aquatic microbial communities. J Microbiol Meth 36:203–213

Chung CT, Niemela SL, Miller RH (1989) One-step preparation of competent *Escherichia coli*: transformation and storage of bacterial cells in the same solution. Proc Natl Acad Sci UAS 86:2172–2175

Colin T, Bories A, Sire Y, Perrin R (2005) Treatment and valorisation of winery wastewater by a new biophysical process (ECCF). Water Sci Technol 51(1):99–106

Cunliffe M, Kertesz MA (2006) Autecological properties of soil sphingomonads involved in the degradation of polycyclic aromatic hydrocarbons. Appl Microbiol Biotechnol 72:1083–1089. doi:10.1007/s00253-006-0374-x

Desai AD, Autenrieth RL, Dimitriou-Christidis P, McDonald JC (2008) Biodegradation kinetics of select polycyclic aromatic hydrocarbon (PAH) mixtures by *Sphingomonas paucimobilis* EPA505. Biodegradation 19:223–233. doi:10.1007/s10532-007-9129-3

Di Gioia D, Fava F, Bertin L, Marchetti L (2001) Biodegradation of synthetic and naturally occurring mixtures of mono-cyclic aromatic compounds present in olive mill wastewaters by two aerobic bacteria. Appl Microbiol Biotechnol 55:619–626. doi:10.1007/s002530000554

Díaz E, Stams AJM, Amils R, Sanz JL (2006) Phenotypic properties and microbial diversity of methanogenic granules from a full-scale upflow anaerobic sludge bed reactor treating brewery wastewater. Appl Environl Microbiol 72(7):4942–4949. doi:10.1128/AEM.02985-05

Dice LR (1945) Measures of the amount of ecologic association between species. Ecology 26(3):297–302

Doaré-Lebrun E, El Arbi A, Charlet M, Guérin L, Pernelles J-J, Ogier J-C, Bouix M (2006) Analysis of fungal diversity of grapes by application of temporal temperature gradient gel electrophoresis–potentialities and limits of the method. J Appl Microbiol 101:1340–1350. doi:10.1111/j.1365-2672.2006.03030.x

Eichner CA, Erb RW, Timmis KN, Wagner-Dobler I (1999) Thermal gradient gel electrophoresis analysis of bioprotection from pollutant shocks in the activated sludge microbial community. Appl Environ Microbiol 65(1):102–109

El Fantroussi S, Agathos SN (2005) Is bioaugmentation a feasible strategy for pollutant removal and site remediation? Curr Opin Microbiol 8:268–275

El Hajjouji H, Bailly JR, Winterton P, Merlina G, Revel JC, Hafidi M (2008) Chemical and spectroscopic analysis of olive mill waste water during a biological treatment. Biores Technol 99:4958–4965. doi:10.1016/j.biortech.2007.09.025

Eusébio A, Petruccioli M, Lageiro M, Federici F, Duarte JC (2004) Microbial characterisation of activated sludge in jet-loop bioreactors treating winery wastewaters. J Ind Microbiol Biotechnol 31:29–34. doi:10.1007/s10295-004-0111-3

Eusébio A, Mateus M, Baeta-Hall L, Almeida-Vara E, Duarte JC (2005) Microflora evaluation of two agro-industrial effluents treated by the JACTO jet-loop type reactor system. Water Sci Technol 51(1):107–112

Eusébio A, Mateus M, Baeta-Hall L, Sàágua MC, Tenreiro R, Almeida-Vara E, Duarte JC (2007) Characterization of the microbial communities in jet-loop (JACTO) reactors during aerobic olive oil wastewater treatment. Internat Biodeter Biodegr 59:226–233. doi:10.1016/j.ibiod.2006.11.008

Garland JL, Mills AL (1991) Classification of heterotrophic microbial communities on the basis of patterns of community level sole-carbon-source utilization. Appl Environ Microbiol 57:2351–2359

George I, Eyers L, Stenuit B, Agathos SN (2008) Effect of 2, 4, 6-trinitrotoluene on soil bacterial communities. J Ind Microbiol Biotechnol 35:225–236. doi:10.1007/s10295-007-0289-2

Guzmán-López O, Loera O, Parada JL, Castillo-Morales A, Martínez-Ramírez C, Augur C, Gaime-Perraud I, Saucedo-Castañeda G (2009) Microcultures of lactic acid bacteria: characterization and selection of strains, optimization of nutrients and gallic acid concentration. J Ind Microbiol Biotechnol 36:11–20. doi:10.1007/s10295-008-0465-z

Hamdi M (1993) Future prospects and constraints of olive mill wastewaters use and treatment: a review. Bioproc Eng 8:209–214. doi:10.1007/BF00369831

Henriques IS, Alves A, Tacão M, Almeida A, Cunha A, Correia A (2006) Seasonal and spatial variability of free-living bacterial community composition along an estuarine gradient (Ria de Aveiro, Portugal). Estuar Coast Shelf Sci 68:139–148. doi:10.1016/j.ecss.2006.01.015

Hill TCJ, Walsh KA, Harris JA, Moffett BF (2003) Using ecological diversity measures with bacterial communities. FEMS Microbiol Ecol 43:1–11

Ito M, Prokop Z, Klvaka M, Otsubo Y, Tsuda M, Damborský J, Nagata Y (2007) Degradation of β-hexachlorocyclohexane by haloalkane dehalogenase LinB from γ-hexachlorocyclohexane-utilizing bacterium *Sphingobium* sp. MI1205. Arch Microbiol 188:313–325. doi:10.1007/s00203-007-0251-8

Kachouri F, Hamdi M (2004) Enhancement of polyphenols in olive oil by contact with fermented olive mill wastewater by *Lactobacillus plantarum*. Process Biochem 39: 841–845. doi:10.1016/S0032-9592(03)00189-4

Kiritsakis A, Koutsaftakis A, Stefanoudaki E, Kostopoulou M, Digenakis M, Polymenopoulos Z (2001) Environment pollution by the waste water of olive oil mills: how to eliminate the problem. J Environ Protection Ecol 2(4):869–873

Kirk JL, Beaudette LA, Hart M, Moutoglis P, Klironomos JN, Lee H, Trevors JT (2004) Methods of studying soil microbial diversity. J Microbiol Methods 58:169–188. doi:10.1016/j.mimet.2004.04.006

Kolehmainen RE, Tiirola M, Puhakka JA (2008) Spatial and temporal changes in actinobacterial dominance in experimental artificial groundwater recharge. Water Res 42:4525–4537. doi:10.1016/j.watres.2008.07.039

Laconi S, Molle G, Cabiddu A, Pompei R (2007) Bioremediation of olive oil mill wastewater and production of microbial biomass. Biodegradation 18:559–566. doi:10.1007/s10532-006-9087-1

Liu W-T, Chanc O-C, Fang HHP (2002) Characterization of microbial community in granular sludge treating brewery wastewater. Water Res 36:1767–1775

Liu ZP, Wang BJ, Liu YH, Liu SJ (2005) *Novosphingobium taihuense* sp. nov., a novel aromatic-compound-degrading bacterium isolated from Taihu Lake, China. Int J Sys Evol Microbiol 55:1229–1232. doi:10.1099/ijs.0.63468-0

Ludwig JA, Reynolds JF (1988) Statistical ecology—a primer on computing and methods. John Wiley and Sons, New York

Massol-Deya AA, Odelson DA, Hickey RF, Tiedje JM (1995) Bacterial community fingerprinting of amplified 16S–23S ribosomal gene sequences and restriction endonuclease analysis (ARDRA). In: Akkeermans ADL, van-Elsas JD, de-Bruijn FJ (eds) Molecular microbial ecology methods. Kluwer Academic Publishing, Boston 3.3. 2: 1–8

Mechichi T, Sayadi S (2005) Evaluating process imbalance of anaerobic digestion of olive mill wastewaters. Proc Biochem 40:139–145. doi:10.1016/j.procbio.2003.11.050

Mekki A, Dhouib A, Sayadi S (2006) Changes in microbial and soil properties following amendment with treated and untreated olive mill wastewater. Microbiol Res 161: 93–101. doi:10.1016/j.micres.2005.06.001

Moura A, Tacão M, Henriques I, Dias J, Ferreira P, Correia A (2009) Characterization of bacterial diversity in two aerated lagoons of a wastewater treatment plant using PCR–DGGE analysis. Microbiol Res 164(5):560–569. doi:10.1016/j.micres.2007.06.005

Muyzer G (1998) Structure, function and dynamics of microbial communities: the molecular biological approach. In: Carvalho GR (ed) Advances in molecular ecology. IOS Press, Amsterdam, Washington, DC, pp 87–117

Muyzer G (1999) DGGE/TGGE a method for identifying genes from natural ecosystems. Curr Opin Microbiol 2:317–322

Muyzer G, Smalla K (1998) Application of denaturing gradient gel electrophoresis (DGGE) and temperature gradient gel electrophoresis (TCGE) in microbial ecology. Antonie van Leeuwenhoek 73:127–141

Muyzer G, de Waal EC, Uitterlinden AG (1993) Profiling of complex microbial populations by denaturing gradient gel electrophoresis analysis of polymerase chain reaction amplified genes coding for 16S rRNA. Appl Environ Microbiol 59:695–700

Nelson KE, Weinel C, Paulsen IT, Dodson RJ, Hilbert H et al (2002) Complete genome sequence and comparative analysis of the metabolically versatile *Pseudomonas putida* KT2440. Environ Microbiol 4(12):799–808

Paixão SM, Santos P, Baeta-Hall L, Tenreiro R, Anselmo AM (2003) Alternative inocula as activated sludge surrogate culture for a toxicity test. Environm Toxicol 18:37–44. doi:10.1002/tox.10099

Pielou EC (1966) The measurement of diversity in different types of biological collections. J Theor Biol 13:131–144

Piperidou CI, Chaidou CI, Stalikas CD, Soulti K, Pilidis GA, Balis C (2000) Bioremediation of olive oil mill wastewater: chemical alterations induced by *Azotobacter vinelandii*. J Agric Food Chem 48:1941–1948. doi:10.1021/jf991060v

Pozo C, Rodelas B, Martínez-Toledo MV, Vílchez R, González-López J (2007) Removal of organic load from olive washing water by an aerated submerged biofilter and profiling of the bacterial community involved in the process. J Microbiol Biotechnol 17(5):784–791

Rincón B, Raposo F, Borja R, Gonzalez JM, Portillo MC, Saiz-Jiménez C (2006) Performance and microbial communities of a continuous stirred tank anaerobic reactor treating two-phases olive mill solid wastes at low organic loading rates. J Biotechnol 121:534–543. doi:10.1016/j.jbiotec.2005.08.013

Rincón B, Borja R, Gonzalez JM, Portillo MC, Saiz-Jiménez C (2008) Influence of organic loading rate and hydraulic

retention time on the performance, stability and microbial communities of one-stage anaerobic digestion of two-phase olive mill solid residue. Biochem Eng J 40: 253–261. doi:10.1016/j.bej.2007.12.019

Ritchie NJ, Schutter ME, Dick RP, Myrold DD (2000) Use of length heterogeneity PCR and fatty acid methyl ester profiles to characterize microbial communities in soil. Appl Environ Microbiol 66(4):1668–1675

Rizzi A, Zucchi M, Borin S, Marzorati M, Sorlini C, Daffonchio D (2006) Response of methanogen populations to organic load increase during anaerobic digestion of olive mill wastewater. J Chem Technol Biotechnol 81: 1556–1562. doi:10.1002/jctb.1558

Saikaly PE, Oerther DB (2004) Bacterial competition in activated sludge: theoretical analysis of varying solids retention times on diversity. Microb Ecol 48:274–284. doi:10.1007/s00248-003-1027-6

Sevilla M, Gunapala N, Burris RH, Kennedy C (2001) Enhancement of growth and N content in sugarcane plants inoculated with *Acetobacter diazotrophicus*. Mol Plant Microbe Interact 14:358–366

Shannon CE, Weaver W (1963) The mathematical theory of communication. University of Illinois Press, Urbana, IL, USA

Smalla K, Tebbe CC, van Elsas JD, Vogel TM (2008) Microbial community networks. FEMS Microbiol Ecol 66:1–2. doi:10.1111/j.1574-6941.2008.00596.x

Sousa DZ, Pereira MA, Stams AJM, Alves MM, Smidt H (2007) Microbial communities involved in anaerobic degradation of unsaturated or saturated long-chain fatty acids. Appl Environ Microbiol 73(4):1054–1064. doi: 10.1128/AEM.01723-06

Stolz A (2009) Molecular characteristics of xenobiotic-degrading sphingomonads. Appl Microbiol Biotechnol 81:793–811. doi:10.1007/s00253-008-1752-3

Talbot G, Topp E, Palin MF, Massé DI (2008) Evaluation of molecular methods used for establishing the interactions and functions of microorganisms in anaerobic bioreactors. Water Res 42:513–537. doi:10.1016/j.watres.2007.08.003

ter Braak CJF, Verdonschot PFM (1995) Canonical correspondence analysis and related multivariate methods in aquatic ecology. Aquat Sci 57:255–289

Tiirola MA, Männistö MK, Puhakka JA, Kulomaa MS (2002) Isolation and characterization of *Novosphingobium* sp. strain MT1, a dominant polychlorophenol-degrading strain in a groundwater bioremediation system. Appl Environ Microbiol 68(1):173–180

Tiirola MA, Suvilampi JE, Kulomaa MS, Rintala JA (2003) Microbial diversity in a thermophilic aerobic biofilm process: analysis by length heterogeneity PCR (LH-PCR). Water Res 37:2259–2269. doi:10.1016/S0043-1354(02)00631-0

Timmis KN (2002) *Pseudomonas putida*: a cosmopolitan opportunist *par excellence*. Environ Microbiol 4(12): 779–781

Tombolini R, Unge A, Davey ME, de Bruijn FJ, Jansson JK (1997) Flow cytometric and microscopic analysis of GFP-tagged *Pseudomonas fluorescens* bacteria. FEMS Microbiol Ecol 22:17–28

Trefault N, De la Iglesia R, Molina AM, Manzano M, Ledger T, Pérez-Pantoja D, Sánchez MA, Stuardo M, González B (2004) Genetic organization of the catabolic plasmid pJP4 from *Ralstonia eutropha* JMP134 (pJP4) reveals mechanisms of adaptation to chloroaromatic pollutants and evolution of specialized chloroaromatic degradation pathways. Environ Microbiol 6(7):655–668. doi:10.1111/j.1462-2920.2004.00596.x

Tsioulpas A, Dimou D, Iconomou D, Aggelis G (2002) Phenolic removal in olive oil mill wastewater by strains of *Pleurotus* spp. in respect to their phenol oxidase (laccase) activity. Biores Technol 84:251–257. doi:10.1016/S0960-8524(02)00043-3

Ude S, Arnold DL, Moon CD, Timms-Wilson T, Spiers AJ (2006) Biofilm formation and cellulose expression among diverse environmental *Pseudomonas* isolates. Environ Microbiol 8(11):1997–2011. doi:10.1111/j.1462-2920.2006.01080.x

Wang J, Ma T, Zhao L, Lv J, Li G, Zhang H, Zhao B, Liang F, Liu R (2008) Monitoring exogenous and indigenous bacteria by PCR-DGGE technology during the process of microbial enhanced oil recovery. J Ind Microbiol Biotechnol 35:619–628. doi:10.1007/s10295-008-0326-9

Watanabe K, Teramoto M, Futamata H, Harayama S (1998) Molecular detection, isolation, and physiological characterization of functionally dominant phenol-degrading bacteria in activated sludge. Appl Environ Microbiol 64(11):4396–4402

Watanabe K, Futamata H, Harayama S (2002) Understanding the diversity in catabolic potential of microorganisms for the development of bioremediation strategies. Antonie van Leeuwenhoek 81:655–663

White DC, Suttont SD, Ringelberg DB (1996) The genus *Sphingomonas:* physiology and ecology. Curr Op Biotechnol 7:301–306

Whiteley AS, Wiles S, Lilley AK, Philp J, Bailey MJ (2001) Ecological and physiological analyses of *Pseudomonad* species within a phenol remediation system. J Microbiol Methods 44:79–88

Zhong Y, Luan T, Wang X, Lan C, Tam NFY (2007) Influence of growth medium on cometabolic degradation of polycyclic aromatic hydrocarbons by *Sphingomonas* sp. strain PheB4. Appl Microbiol Biotechnol 75:175–186. doi: 10.1007/s00253-006-0789-4

Zhou J, Bruns MA, Tiedje JM (1996) DNA recovery from soils of diverse composition. Appl Environ Microbiol 62:316–322